Rare Met. (2022) 41(12):4273–4278
https://doi.org/10.1007/s12598-016-0816-2

RARE METALS
www.editorialmanager.com/rmet

Microwave-hydrothermal synthesis, characterization and upconversion luminescence of rice-like $Gd(OH)_3$ nanorods

Shuang Huang, Hua-Lan Xu, Lei Wang, Sheng-Liang Zhong*

Received: 2 October 2015 / Revised: 1 December 2015 / Accepted: 4 November 2016 / Published online: 20 December 2016

Abstract Rice-like $Gd(OH)_3$ nanorods were successfully prepared through a facile and rapid microwave-hydrothermal synthesis method without using any surfactants or templates. X-ray diffraction (XRD), Fourier transform infrared (FTIR) spectroscopy, thermogravimetric analysis (TGA), scanning electron microscopy (SEM), transmission electron microscopy (TEM), high-resolution transmission electron microscopy (HRTEM), selected area electron diffraction (SAED) and energy-dispersive spectroscopy (EDS) were used to characterize the samples. Results show that the nanorods have an average length of 400 nm and an average diameter of 50 nm. The effects of reaction parameters such as reaction temperature and time on the preparation were briefly investigated. It is found that the crucial factor for the formation of rice-like $Gd(OH)_3$ nanorods is reaction time. When the rice-like $Gd(OH)_3$ nanorods was codoped with Yb^{3+} and Er^{3+}, strong upconversion emissions could be observed under the excitation of 980-nm-laser, and the calculated CIE color coordinates falls within the yellow region, which may be potential candidate for optical materials.

Keywords Microwave-hydrothermal synthesis; Gadolinium hydroxide; Upconversion; Rare earth

1 Introduction

At present, lanthanum hydroxides and their oxides or dehydroxides are widely applied in various fields, including as electronic, magnetic, optical materials, superconductive materials, catalyst, etc. [1–3]. Gadolinium hydroxide ($Gd(OH)_3$), one of the important lanthanide hydroxides candidates, which has been used in biomedical, luminescent and catalytic fields, has attracted much attention to conduct research on it [4–9]. To date, many methods have been developed to prepare $Gd(OH)_3$, ranging from conventional hydrothermal treatment [10–13], coprecipitation [14], sol–gel process [15], combustion [16], template method [17], and wet-chemical route [18]. A variety of morphologies, such as nanorods, nanobundles, nanotubes, nanoparticles, nanosheets, hollow spheres, nanoflowers, nanoclusters, nanowires, etc. [8, 18–23], have been reported by many researchers. Gadolinium oxide (Gd_2O_3) was generally prepared by high temperature thermal annealing of $Gd(OH)_3$. When doped with fluorescent ions, such as Eu^{3+}, Yb^{3+}, Er^{3+}, Pr^{3+}, and Tm^{3+}, they can be as important emitting phosphors, which are promising luminescent materials applied in novel optoelectronic devices [24–27].

Compared to above methods, microwave synthesis possesses fast, uniform heating, eco-friendly and energy-efficient characteristics [28]. Meanwhile, microwave chemistry has advantages of voluminal heating, high energy efficiency and reaction selectivity, which is widely used in all kinds of fields of synthetic chemistry. It was proved that products could be obtained in short reaction time and high reaction rate by microwave way [29]. Straw-sheaf-like terbium-based coordination polymer architectures and coordination polymer submicrospheres were obtained successfully via microwave heating method [30, 31].

Recently, great effort has been put on the controlled synthesis of one-dimensional (1D) nanomaterials with unique properties, especially rod-like nanomaterials with

S. Huang, H.-L. Xu, L. Wang, S.-L. Zhong*
College of Chemistry and Chemical Engineering, Jiangxi Normal University, Nanchang 330022, China
e-mail: slzhong@jxnu.edu.cn

morphology-dependent performance [32–35]. However, $Gd(OH)_3$:Yb/Er 1D nanomaterials were seldom investigated. Photoluminescence study for Yb^{3+}, Er^{3+} doped in $Gd(OH)_3$ nanorods will be helpful to further highlight the photoluminescence profiles, as well as to understand the mechanism of luminescent materials. In this work, a fast and simple microwave-hydrothermal synthesis method [36] was presented for the fabrication of well-defined rice-like nanorods. When codoped with Yb^{3+} and Er^{3+}, upconversion emission was realized in the $Gd(OH)_3$:Yb/Er nanorods. This method may be employed in the preparation of other lanthanide hydroxides.

2 Experimental

2.1 Chemicals and instruments

$RE(NO_3)_3{\cdot}6H_2O$ (RE = Gd^{3+}/Yb^{3+}/Er^{3+}, 99.99%) were purchased from Shanghai Aladdin Industrial Corporation. NaOH was provided by Tianjing Fuchen Chemical Reagents Factory. All chemical agents were of analytical grade and used directly without further purification.

The MDS-6G microwave reactor system (Shanghai Sineo Microwave Chemistry Technology Co., Ltd., China) was used for the synthesis of $Gd(OH)_3$. The crystalline phase was identified by a Rigaku X-ray diffractometer (XRD) with Cu Kα radiation ($\lambda = 0.154178$ nm). The morphologies of the products were observed by scanning electron microscopy (SEM, Hitachi, S-3400 N) equipped with energy-dispersive spectroscopy (EDS). The morphologies and sizes of the samples were taken by a transmission electron microscopy (TEM, JEM-2100, Japan) under an acceleration voltage of 200 kV. Fourier transform infrared spectroscopy (FTIR, Perkin-Elmer) was recorded in a KBr pellet in the spectral range of 4000–400 cm^{-1} at room temperature. Thermogravimetric (TG) and differential thermal analysis (DTA) were carried out under atmosphere on a TA-50 thermal analyzer from 20 to 800 °C, with a heating rate of 10 °C·min^{-1}. Upconversion luminescence was tested by an FLS 980 (Edinburgh Instruments, England) equipped with a 980-nm-laser diode.

2.2 Preparation of $Gd(OH)_3$

The rice-like $Gd(OH)_3$ nanorods were fabricated by a microwave-hydrothermal method. In a representative synthesis route, $Gd(NO_3)_3{\cdot}6H_2O$ (1 mmol) was dissolved in 25 ml deionized water. Next, some amount of aqueous NaOH solution was added drop-wise to the above solution under stirring until the pH was adjusted to 12. Finally, the mixture was placed in Teflon-lined reaction vessel and maintained at 120 °C for 1 h employing a microwave power of 300 W. The reaction vessel was cooled naturally to room temperature. The obtained white precipitations ($Gd(OH)_3$) were washed with deionized water and ethanol several times and dried in vacuum at 60 °C for 24 h. Similarly, $Gd(OH)_3$:Yb/Er samples were prepared via the above procedure just by using the corresponding $RE(NO_3)_3{\cdot}6H_2O$ (Gd^{3+}/Yb^{3+}/Er^{3+}).

3 Results and discussion

Figure 1 shows XRD pattern of typical sample. All diffraction peaks are readily indexed to be pure hexagonal $Gd(OH)_3$, which agrees very well with the standard values of $Gd(OH)_3$ (JCPDS No. 83-2037). These high and sharp patterns, with no characteristic peaks of other crystalline phases, indicate that the products are pure and well crystallized. The sharp peaks correspond to (100), (110), (101), (201), (211) planes of hexagonal crystalline $Gd(OH)_3$ phase.

SEM images of typical sample synthesized by microwave-hydrothermal method are shown in Fig. 2a, b, giving rice-like morphology with diameter of about 50 nm and length of about 400 nm. It was reported that $Gd(OH)_3$ nanorods prepared by hydrothermal method could be attributed to rapid growth along [001] direction [12]. HRTEM image of $Gd(OH)_3$ nanorods, as shown in Fig. 2c, clearly shows that lattice fringes with a spacing of 0.31 nm correspond to the (110) planes of hexagonal-phase $Gd(OH)_3$. SAED pattern obtained on an individual nanorod is shown in Fig. 2d. They appear as rings patterns, specified as single crystal of $Gd(OH)_3$ nanorods in nature. These rings are indexed as (100), (110), (200), (201) and (211) reflection planes of $Gd(OH)_3$ nanorods with [111] zone axis, in agreement with the corresponding XRD results.

Figure 3 shows FTIR spectra of typical product. Board band at 3100–3550 cm^{-1} corresponds to O–H stretching vibration of adsorbed water molecule in $Gd(OH)_3$. Sharp

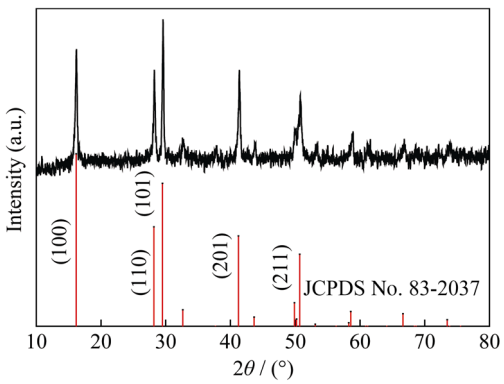

Fig. 1 XRD pattern of typical product

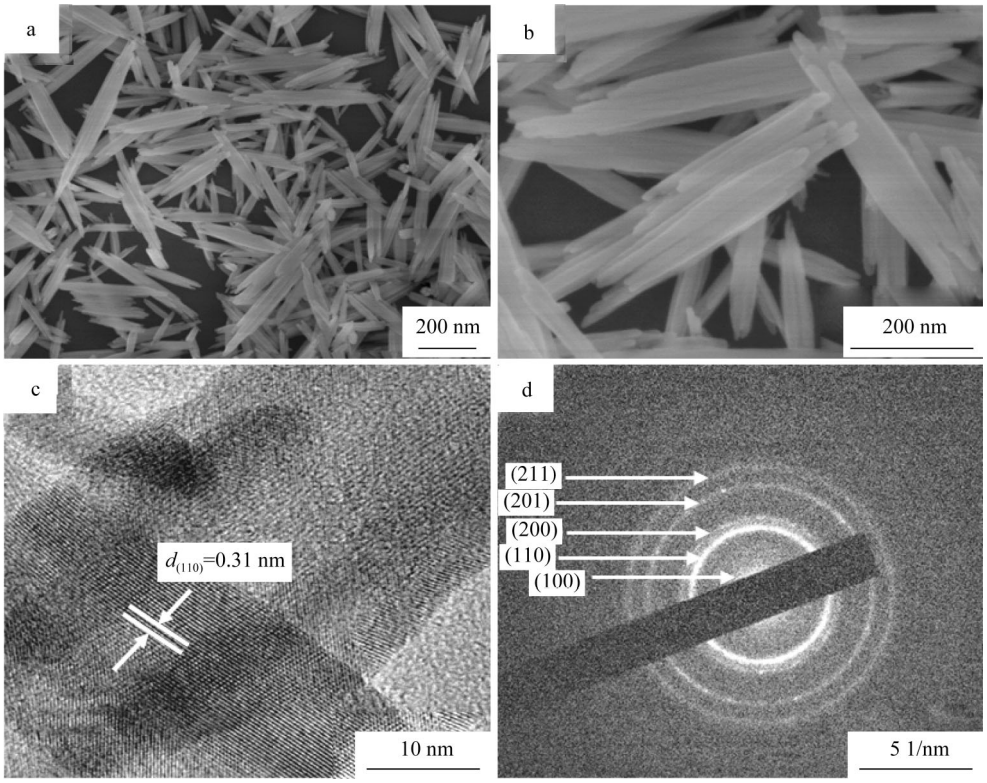

Fig. 2 Microstructures of typical product: **a**, **b** SEM images, **c** HRTEM image, and **d** SAED pattern

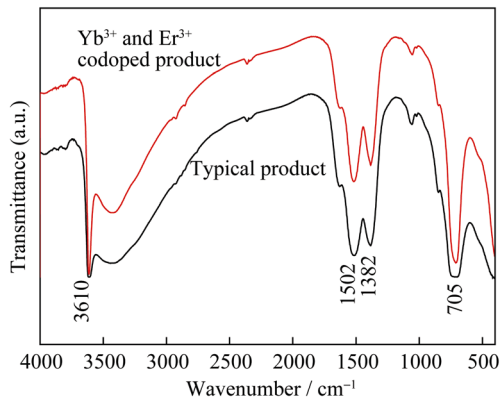

Fig. 3 FTIR spectra of typical product and Yb^{3+} and Er^{3+} codoped product

intense bands at 705 and 3610 cm^{-1} are assigned to be Gd–O–H bending [36]. Two peaks are commonly observed at 1382 and 1502 cm^{-1}, attributed to symmetric and asymmetric stretching of COO^-, respectively [37]. EDS results indicate the presence of Gd and O elements in $Gd(OH)_3$ nanorods (Fig. 4a). When codoped with Yb^{3+} and Er^{3+} (Fig. 4b), no elements other than Gd, O, Yb and Er are present (H element cannot be detected by EDS), which demonstrates that Yb^{3+} and Er^{3+} have been successfully codoped in nanorods. Furthermore, EDS spectrum shows an approximate atomic ratio of 1:3 for (Gd, Yb, Er):O, which matches well with that of $Gd(OH)_3$ within experimental error of EDS. EDS analysis gives further support for XRD results.

TG/DTA (Fig. 5) was used to determine the annealing temperature of $Gd(OH)_3$ dehydration into the final Gd_2O_3 powder. The curves show weight loss in three steps between room temperature and 800 °C in nitrogen gas atmosphere. Initially, a very gradual decrease in weight (4.31%) is observed between room temperature and 232 °C, due to the dehydration of physically adsorbed H_2O in $Gd(OH)_3$. The second step starts from 232 up to 305 °C, resulted from a dehydration process: $2Gd(OH)_3 \rightarrow 2GdOOH + 2H_2O$ [18, 36], with the weight loss of 8.58%. The third step is caused by the further decomposition of GdOOH to Gd_2O_3 at 305–426 °C (weight loss of 3.54%), where GdOOH converts into Gd_2O_3 via a reaction of 2GdOOH–$Gd_2O_3 + H_2O$ [18, 36]. It is observed a total weight loss of 16.43% for $2Gd(OH)_3 \rightarrow Gd_2O_3 + 3H_2O$. No critical change in weight is observed between 700 and 800 °C, indicating a thermal stability of Gd_2O_3 up to 1000 °C. As discussed above, it is obtained the cubic Gd_2O_3 crystal phase upon thermal annealing at 700 °C. The total weight loss of $Gd(OH)_3$ is 12.12%, in good accordance with the decomposition of $Gd(OH)_3$ to Gd_2O_3 obtained by theoretical calculation (12.97%).

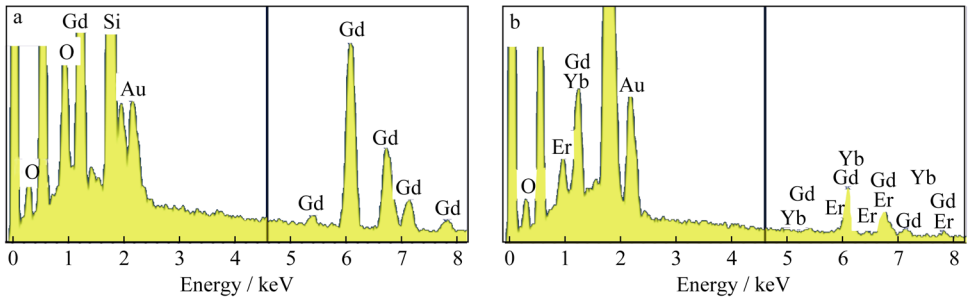

Fig. 4 EDS spectra of **a** typical product and **b** Yb^{3+} and Er^{3+} codoped product

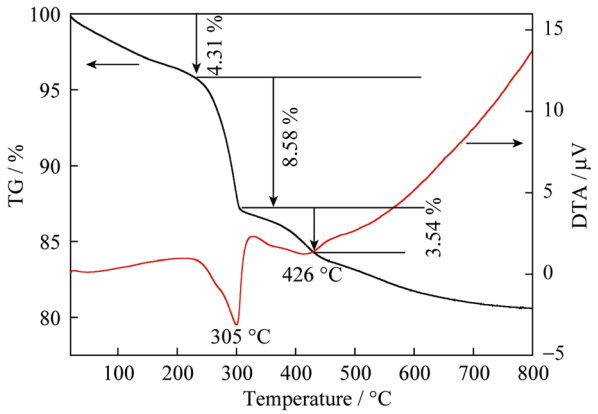

Fig. 5 TG/DTA curves of typical product

To determine the effect of reaction time on the formation of the rice-like $Gd(OH)_3$ nanorods while retaining other reaction conditions unchanged, SEM images obtained at 120 °C are shown in Fig. 6. It is obvious that the morphology changes greatly with different reaction time. At 30 min, rice-like nanorods were not fully formed (Fig. 6a). Interestingly, with the increase of reaction time to 60 min, a large amount of nanorods with an average length of 400 nm and an average diameter of 50 nm are obtained (Fig. 2b). No obvious change is observed in the products when the reaction time is prolonged to 90 min or longer (120 min) (Fig. 6b, c). The effect of reaction temperature on the preparation of rice-like $Gd(OH)_3$ nanorods were also investigated, a series of experiments were carried out at 100, 140 and 160 °C for 60 min with other conditions being the same. All the products are found to be rice-like nanorods (Fig. 7), illuminating that the reaction temperature has slight effect on the formation of rice-like $Gd(OH)_3$ nanorods. Based on above results, it can be concluded that the crucial factor for the formation of rice-like $Gd(OH)_3$ nanorods through microwave-hydrothermal synthesis method is reaction time.

Figure 8 displays upconversion emission spectrum of Er^{3+}/Yb^{3+} codoped $Gd(OH)_3$ nanorods at room temperature. The spectrum is composed of two parts. Under 980-nm-excitation, the weak peaks in the green emission regions of 522–539 and 548–563 nm are assigned to $^2H_{11/2}$, $^4S_{3/2}$–$^4I_{15/2}$ transitions of Er^{3+}, respectively. A strong red emission near 661 nm comes from $^4F_{9/2}$–$^4I_{15/2}$ transition in rice-like $Gd(OH)_3$:Yb/Er nanorods. To measure the color of visible emissions that the naked eye perceived, the chromaticity coordinates are calculated from the spectra by the method using 1931 CIE (Commission Internationale de I'Eclairage France) system. The calculated CIE color coordinates (0.466, 0.519) fall within the yellow region.

From the upconversion (UC) spectrum, one knows that both $^2H_{11/2}$–$^4I_{15/2}$ and $^4S_{3/2}$–$^4I_{15/2}$ transitions are split into two peaks. Under 980-nm-excitation, Yb^{3+} is excited to $^2F_{5/2}$ level from ground state. Then the energy is transferred to adjacent Er^{3+}, leading to the population of $^4I_{11/2}$ level. At the same time, the multiphonon relaxation occurs and part of $^4I_{11/2}$ level decays to $^4I_{13/2}$ level [38]. During the lifetime of $^4I_{11/2}$ and $^4I_{13/2}$ levels, the second photon energy is absorbed by Yb^{3+} and again the energy is transferred to Er^{3+}. Subsequently, electrons located at $^4F_{7/2}$ level nonradiatively relax to $^2H_{11/2}$, $^4S_{3/2}$ and $^4F_{9/2}$ levels [39]. Finally,

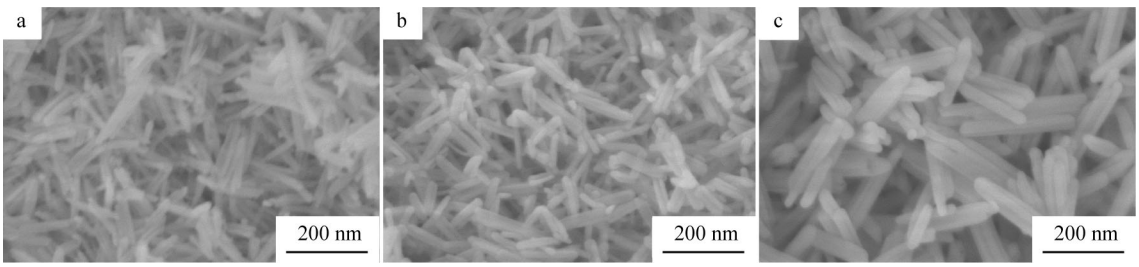

Fig. 6 SEM images of rice-like $Gd(OH)_3$ nanorods obtained at 120 °C for different time: **a** 30 min, **b** 90 min, and **c** 120 min

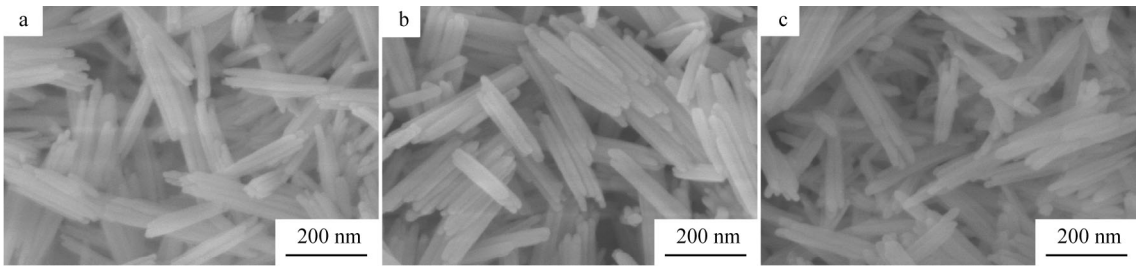

Fig. 7 SEM images of rice-like $Gd(OH)_3$ nanorods obtained at different temperatures for 60 min: **a** 100 °C, **b** 140 °C, and **c** 160 °C

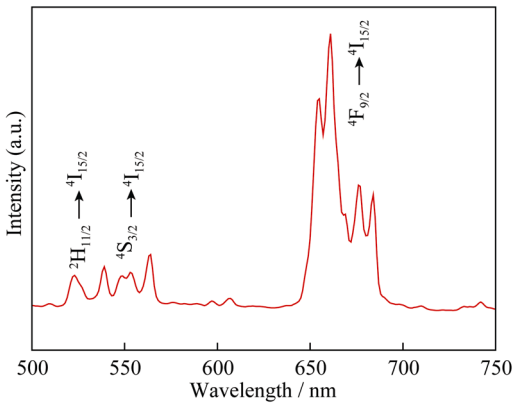

Fig. 8 Upconversion emission spectrum of Er^{3+}/Yb^{3+}-codoped $Gd(OH)_3$ nanorods at room temperature under 980-nm-excitation

these electrons relax to the ground state $^4I_{15/2}$, leading to the green and red upconversion emission. While the red emission of $^4F_{9/2}$–$^4I_{15/2}$ is stronger than the green emissions of $^2H_{11/2}$, $^4S_{3/2}$–$^4I_{15/2}$ in the rice-like $Gd(OH)_3$:Yb/Er nanorods, hence the sample presents to be yellow.

4 Conclusion

In summary, rice-like $Gd(OH)_3$ nanorods were successfully fabricated via a fast and facile microwave-hydrothermal route. Results demonstrate that the products have an average length of 400 nm and an average diameter of 50 nm. It turns out that the crucial factor for the formation of rice-like $Gd(OH)_3$ nanorods through microwave-hydrothermal synthesis method is reaction time, while the reaction temperature has slight effect on the formation of rice-like $Gd(OH)_3$ nanorods. When doped with Yb^{3+} and Er^{3+}, the rice-like $Gd(OH)_3$:Yb/Er nanorods show strong upconversion emissions under the excitation of 980-nm-laser. The calculated CIE color coordinates of rice-like $Gd(OH)_3$ nanorods fall well within the yellow region, which may expand their application from optics to the biological field. This method has the advantages of time saving, uniform heating, high purity and quality. Also it is eco-friendly and energy-efficient, which holds promise in the preparation of other rare earth nanostructures facilely.

Acknowledgements This study was financially supported by the National Natural Science Foundation of China (Nos. 21201089, 21261010 and 61201104), Jiangxi Provincial Education Department (No. KJLD13021) and Jiangxi Provincial Department of Science and Technology (Nos. 20144BCB23039 and 20151BDH80049).

References

[1] Wang Y, Liu S, Cai Y, Deng S, Han B, Han R, Li Q, Wang Y. $La(OH)_3:Ln^{3+}$ (Ln = Sm, Er, Gd, Dy, and Eu) nanorods synthesized by a facile hydrothermal method and their enhanced photocatalytic degradation of Congo red in the aqueous solution. Ceram Int. 2014;40(3):5091.

[2] Liu S, Cai Y, Cai X, Li H, Zhang F, Mu Q, Liu Y, Wang Y. Catalytic photodegradation of Congo red in aqueous solution by $Ln(OH)_3$ (Ln = Nd, Sm, Eu, Gd, Tb, and Dy) nanorods. Appl Catal A Gen. 2013;453(6):45.

[3] Mu Q, Wang Y. A simple method to prepare $Ln(OH)_3$ (Ln = La, Sm, Tb, Eu, and Gd) nanorods using CTAB micelle solution and their room temperature photoluminescence properties. J Alloys Compd. 2011;509(5):2060.

[4] Kim WJ, Gwag JS, Kang JG, Sohn Y. Photoluminescence imaging of Eu(III), Eu(III)/Ag, Eu(III)/Tb(III), and eualli-pab(III)/Ag-doped $Gd(OH)_3$ and Gd_2O_3 nanorods. Ceram Int. 2014;40(8):12035.

[5] Yang Y, Sun Y, Liu Y, Peng J, Wu Y, Zhang Y, Feng W, Li F. Long-term in vivo biodistribution and toxicity of $Gd(OH)_3$ nanorods. Biomaterials. 2013;34(2):508.

[6] Padhi DK, Pradhan GK, Parida KM, Singh SK. Facile fabrication of $Gd(OH)_3$ nanorod/RGO composite: synthesis, characterisation and photocatalytic reduction of Cr(VI). Chem Eng J. 2014;255(7):78.

[7] Chen HY, Zhang JH, Wang XJ, Gao SY, Zhang MZ, Ma YM, Dai QQ, Li DM, Kan SH, Zou GT. The effect of the size of raw $Gd(OH)_3$ precipitation on the crystal structure and PL properties of Gd_2O_3:Eu. J Colloid Interface Sci. 2006;297(1):130.

[8] Yang Y, Zhang QC, Pan YY, Long LS, Zheng LS. Magnetocaloric effect and thermal conductivity of $Gd(OH)_3$ and $Gd_2O(OH)_4(H_2O)_2$. Chem Commun. 2015;51(34):7317.

[9] Hu KW, Hsu KC, Yeh CS. pH-Dependent biodegradable silica nanotubes derived from $Gd(OH)_3$ nanorods and their potential for oral drug delivery and MR imaging. Biomaterials. 2010;31(26):6843.

[10] Kang JG, Min BK, Sohn Y. Synthesis and characterization of $Gd(OH)_3$ and Gd_2O_3 nanorods. Ceram Int. 2015;41(1):1243.

[11] Ruan H, Liu B, Li H. Controlled synthesis of graphene-$Gd(OH)_3$ nanocomposites and their application for detection of ascorbic acid. RSC Adv. 2015;5(27):21242.
[12] Du GH, Van Tendeloo G. Preparation and structure analysis of $Gd(OH)_3$ nanorods. Nanotechnology. 2005;16(4):595.
[13] Yin YD, Hong GY, Xin BF. Preparation and characterization of gadolinium hydroxide single-crystalline nanorods by a hydrothermal process. Chin Chem Lett. 2007;18(4):491.
[14] Li G, Liang Y, Zhang M, Yu D. Size-tunable synthesis and luminescent properties of $Gd(OH)_3$:Eu^{3+} and Gd_2O_3:Eu^{3+} hexagonal nano-/microprisms. Cryst Eng Comm. 2014;16(29): 6670.
[15] Jia Y, Song Y, Bai Y, Wang Y. Upconverted photoluminescence in Ho^{3+} and Yb^{3+} codoped Gd_2O_3 nanocrystals with and without Li^+ ions. Luminescence. 2011;26(4):259.
[16] Kumar RGA, Hata S, Gopchandran KG. Diethylene glycol mediated synthesis of Gd_2O_3:Eu^{3+} nanophosphor and its Judd–Ofelt analysis. Ceram Int. 2013;39(8):9125.
[17] Gao Y, Zhao Q, Fang Q, Xu Z. Facile fabrication and photoluminescence properties of rare-earth-doped Gd_2O_3 hollow spheres via a sacrificial template method. Dalton Trans. 2013; 42(31):11082.
[18] Jia G, Liu K, Zheng Y, Song Y, Yang M, You H. Highly uniform $Gd(OH)_3$ and Gd_2O_3:Eu^{3+} nanotubes: facile synthesis and luminescence properties. J Phys Chem C. 2009;113(15):6050.
[19] Park JY, Kattel K, Xu W, Kim HG, Lee EJ, Lee GH, Lee JJ, Chang Y, Kim TJ. Longitudinal water proton relaxivities of $Gd(OH)_3$ nanorods, $Gd(OH)_3$ nanoparticles, and Gd_2O_3 nanoparticles: dependence on particle diameter, composition, and morphology. J Korean Phys Soc. 2011;59(3):2376.
[20] Yin Y, Hong G. Synthesis and characterization of $Gd(OH)_3$ nanobundles. J Nanoparticle Res. 2006;8(5):755.
[21] Singh V, Naka T, Takami S, Sahraneshin A, Togashi T, Aoki N, Hojo D, Arita T, Adschiri T. Hydrothermal synthesis of inorganic–organic hybrid gadolinium hydroxide nanoclusters with controlled size and morphology. Dalton Trans. 2013;42(45): 16176.
[22] Wang PP, Bai B, Huang L, Hu S, Zhuang J, Wang X. General synthesis and characterization of a family of layered lanthanide (Pr, Nd, Sm, Eu, and Gd) hydroxide nanowires. Nanoscale. 2011;3(6):2529.
[23] Lee KH, Lee BI, You JH, Byeon SH. Transparent Gd_2O_3:Eu phosphor layer derived from exfoliated layered gadolinium hydroxide nanosheets. Chem Commun. 2010;46(9):1461.
[24] Wang JX, Liu L, Dong XT, Liu GX. Fabrication and characterization of Gd_2O_3:Yb^{3+}, Er^{3+} upconversion nanofibers. J Infrared Millim Waves. 2010;29(1):10.
[25] Jin Y, Chen S, Duan J, Jia G, Zhang J. Europium-doped Gd_2O_3 nanotubes cause the necrosis of primary mouse bone marrow stromal cells through lysosome and mitochondrion damage. J Inorg Biochem. 2015;146:28.
[26] Vu HHT, Atabaev TS, Kim YD, Lee JH, Kim HK, Hwang YH. Synthesis and optical properties of Gd_2O_3:Pr^{3+} phosphor particles. J Sol Gel Sci Technol. 2012;64(1):156.
[27] Wu X, Hu S, Tan C, Liu Y. Enhanced red luminescence in Gd_2O_3:Eu^{3+}, Sm^{3+} and its dependence on temperature. Opt Commun. 2014;328(10):23.
[28] Baig RBN, Varma RS. Alternative energy input: mechanochemical, microwave and ultrasound-assisted organic synthesis. Chem Soc Rev. 2012;41(4):1559.
[29] Kitchen HJ, Vallance SK, Kennedy JL, Tapia-Ruiz N, Carassiti L, Harrison A, Whittaker AG, Drysdale TD, Kingman SW, Gregory DH. Modern microwave methods in solid-state inorganic materials chemistry: from fundamentals to manufacturing. Chem Rev. 2014;114(2):1170.
[30] Zhong SL, Jing HY, Li Y, Yin S, Zeng CH, Wang L. Strawsheaf-like terbium-based coordination polymer architectures: microwave-assisted synthesis and their application as selective luminescent probes for heavy metal ions. New J Chem. 2015; 39(4):2973.
[31] Zhong S, Jing H, Li Y, Yin S, Zeng C, Wang L. Coordination polymer submicrospheres: fast microwave synthesis and their conversion under different atmospheres. Inorg Chem. 2014; 53(16):8278.
[32] Phuruangrat A, Thongtem T, Thongtem S. Sonochemical synthesis and characterization of uniform lanthanide orthophosphate ($LnPO_4$, Ln = La and Ce) nanorods. Rare Met. 2015; 34(5):301.
[33] Du X, Zhang D, Shi L, Gao R, Zhang J. Morphology dependence of catalytic properties of Ni/CeO_2 nanostructures for carbon dioxide reforming of methane. J Phys Chem C. 2012; 116(18):10009.
[34] Gao R, Zhang D, Maitarad P, Shi L, Rungrotmongkol T, Li H, Zhang J, Cao W. Morphology-dependent properties of MnO_x/ZrO_2-CeO_2 nanostructures for the selective catalytic reduction of NO with NH_3. J Phys Chem C. 2013;117(20):10502.
[35] Yan T, Zhang D, Shi L, Li H. Facile synthesis, characterization, formation mechanism and photoluminescence property of Eu_2O_3 nanorods. J Alloys Compd. 2009;487(1–2):483.
[36] Thongtem T, Phuruangrat A, Ham DJ, Lee JS, Thongtem S. Controlled Gd_2O_3 nanorods and nanotubes by the annealing of $Gd(OH)_3$ nanorod and nanotube precursors and self-templates produced by a microwave-assisted hydrothermal process. Cryst Eng Comm. 2010;12(10):2962.
[37] Kang JG, Jung Y, Min BK, Sohn Y. Full characterization of $Eu(OH)_3$ and Eu_2O_3 nanorods. Appl Surf Sci. 2014;314:158.
[38] Zheng K, Zhang D, Zhao D, Liu N, Shi F, Qin W. Bright white upconversion emission from Yb^{3+}, Er^{3+}, and Tm^{3+}-codoped Gd_2O_3 nanotubes. Phys Chem Chem Phys. 2010;12(27):7620.
[39] Yi Z, Wen B, Qian C, Wang H, Rao L, Liu H, Zeng S. Intense red upconversion emission and shape controlled synthesis of Gd_2O_3:Yb/Er nanocrystals. Adv Condens Matter Phys. 2013;4:1.